THE JOURNAL OF BIOLOGICAL CHEMISTRY VOL. 291, NO. 45, pp. 23477–23488, November 4, 2016

Polypeptide *N*-Acetylgalactosaminyltransferase 13 Contributes to Neurogenesis via Stabilizing the Mucin-type *O*-Glycoprotein Podoplanin*

Received for publication, June 17, 2016, and in revised form, September 6, 2016 Published, JBC Papers in Press, September 14, 2016, DOI 10.1074/jbc.M116.743955

Yingjiao Xu, Wenjie Pang, Jishun Lu, Aidong Shan, and Yan Zhang[1]

From the Ministry of Education Key Laboratory of Systems Biomedicine, Shanghai Center for Systems Biomedicine, Shanghai Jiao Tong University, 800 Dong Chuan Road, Shanghai 200240, China

Mucin-type *O*-glycosylation is initiated by an evolutionarily conserved family of polypeptide *N*-acetylgalactosaminyltransferases (ppGalNAc-Ts). Previously, it was reported that ppGalNAc-T13 is restrictively expressed at a high level in the brain. Here we provide evidence for the critical role of ppGalNAc-T13 in neural differentiation. In detail, we show that the expression of ppGalNAc-T13 was dramatically up-regulated during early neurogenesis in mouse embryonic brains. Similar changes were also observed in cell models of neuronal differentiation by using either primary mouse cortical neural precursor cells or murine embryonal carcinoma P19 cells. Knockout of ppGalNAc-T13 in P19 cells suppressed not only neural induction but also neuronal differentiation. These effects are at least partly mediated by the mucin-type *O*-glycoprotein podoplanin (PDPN), as knockdown of PDPN led to a similar inhibition of neuronal differentiation and PDPN was significantly reduced at the posttranscriptional level after ppGalNAc-T13 knockout. Further data demonstrate that PDPN acts as a substrate of ppGalNAc-T13 and that the ppGalNAc-T13-mediated *O*-glycosylation on PDPN is important for its stability. Taken together, this study suggests that ppGalNAc-T13 contributes to neuronal differentiation through glycosylating and stabilizing PDPN, which provides insights into the regulatory roles of *O*-glycosylation in mammalian neural development.

Development of the CNS involves a well ordered generation of a variety of distinct neural cell types with progressive restriction in fate potential of neural progenitors (1). This process is precisely regulated by a large set of transcriptional factors (2, 3) and occurs with the reorchestration of molecule expression on the cell surface. These molecules, as indicated by many previous reports, include not only various glycoproteins or glycolipids but also the glycans on them (4–6). Accumulating evidence shows that cell surface glycans play crucial roles in CNS development, where they do not function independently but via regulating the functions of their carrier proteins or lipids. It has been reported that *N*-glycans modulate neural cell adhesion, axonal targeting, neural transmission, and neurite outgrowth by affecting the folding or trafficking of certain carrier glycoproteins such as synaptic vesicle protein 2 (SV2) and ionotropic glutamate receptors (7). Also, genetic inactivation of ST8Sia II and ST8Sia IV sialyltransferases, which catalyze polysialic acid structures on neural cell adhesion molecule, leads to severe defects in neurite outgrowth, synaptic plasticity, etc. (7). In contrast to the increasing evidence for the significance of sialylation and *N*-glycosylation, there is very limited information regarding the mechanistic roles of *O*-glycosylation in neural development (8).

Mucin type *O*-glycosylation is an evolutionarily conserved protein modification that plays important roles in protein processing, secretion, stability, and ligand binding (9, 10). In mammals, it is initiated by a family of 20 UDP-GalNAc:polypeptide *N*-acetylgalactosaminyltransferase (ppGalNAc-Ts,[2] EC 2.4.1.41) (11–14), which transfer GalNAc to the hydroxyl group of serine or threonine, forming an α-anomeric linkage. ppGalNAc-Ts display tissue-specific expression in mammals and, notably, unique spatial and temporal patterns of expression during eukaryotic development as well (15). The correct timing of their expression is crucial for proper development, as aberrant expression has been associated with many developmental disorders and multiple diseases (16–27). As examples, ppGalNAc-T1-deficient mice exhibit a developmental delay of the submandibular gland and reduced secretion of basement membrane components (19). ppGalNAc-T2 has been reportedly involved in abnormalities of lipid metabolism (23, 24), at least partly by modulating the proprotein processing of angiopoietin-like protein 3 (ANGPTL3) (25). Unlike the ubiquitous expression of ppGalNAc-T1 and T2, our group has reported that ppGalNAc-T13 is an enzyme restrictively expressed at a high level in the brain, although it shares 84% amino acid identity with ppGalNAc-T1 (28). This prompted us to investigate the role of ppGalNAc-T13 in neural development.

In this study, we show that ppGalNAc-T13 was dramatically up-regulated during neurogenesis in the mouse embryonic

* This work was supported by National Basic Research Program of China Grant 2012CB822103, National High Technology Research and Development Program of China Grant 2012AA020203, National Natural Science Foundation Grants 30970642, 31170771, 31370806, and 31570796, and Specialized Research Fund for the Doctoral Program of Higher Education Grant 20130073110088. The authors declare that they have no conflicts of interest with the contents of this article.

[1] To whom correspondence should be addressed: Shanghai Center for Systems Biomedicine, Shanghai Jiao Tong University, 800 Dongchuan Rd., Shanghai 200240, China. Tel./Fax: 86-21-34206778; E-mail: yanzhang2006@sjtu.edu.cn.

[2] The abbreviations used are: ppGalNAc-T, polypeptide *N*-acetylgalactosaminyltransferase; PDPN, podoplanin; qRT-PCR, quantitative RT-PCR; E, embryonic day; P, postnatal day; ATRA, all-*trans* retinoic acid; CHX, cycloheximide; NC, negative control; GFAP, glial fibrillary acidic protein; CRISPR/Cas9, cluster regularly interspaced short palindromic repeats/CRISPR associated protein 9.

brain and persisted at a high level after birth. Knockout of ppGalNAc-T13 in murine embryonal carcinoma P19 cells not only reduced the aggregate size of neural stem cells but also inhibited neuronal differentiation. These effects of ppGalNAc-T13 are at least partly mediated by podoplanin (PDPN), a classical mucin-type *O*-glycoprotein, as further data show that the expression of PDPN was significantly down-regulated in ppGalNAc-T13 knockout cells; that, like ppGalNAc-T13 knockout, depletion of PDPN expression also resulted in an inhibition of neuronal differentiation; and that the ppGalNAc-T13-mediated *O*-glycosylation on PDPN is required for its stability. Taken together, our results clearly demonstrate that ppGalNAc-T13 contributes to neuronal differentiation by regulating the stability of PDPN, which provides a plausible explanation for its restrictive expression in the brain.

Results

The Expression of ppGalNAc-T13 Is Dramatically Up-regulated during Neurogenesis—Consistent with our previous study (28) in humans, quantitative RT-PCR (qRT-PCR) analysis with different murine tissues here also revealed high expression of *ppGalNAc-T13* in the brain (Fig. 1*A*), suggesting a possible role of ppGalNAc-T13 in the nervous system. To test this idea, we first examined its expression during the embryonic and postnatal development of the mouse brain. In contrast to the persistently high level during the postnatal period, qRT-PCR results showed that *ppGalNAc-T13* transcription in the embryonic stage was initially increased and peaked at embryonic day 17.5 (E17.5), followed by a momentary decrease at E19.5 (Fig. 1*B*). Because ppGalNAc-T1 shares 84% identity with ppGalNAc-T13, we also detected the expression of ppGalNAc-T1 during brain development. Interestingly, unlike the dramatic increase of ppGalNAc-T13, ppGalNAc-T1 was persistently highly expressed and had little change during the process (Fig. 1*B*).

To confirm the changes of *ppGalNAc-T13* during brain development, an *in vitro* model of progressive neuronal differentiation was established using cortical neural precursor cells isolated from E17.5 mouse brain. Neurite formation and neuronal interactions were gradually up-regulated during the maturation of primary neuronal cells (Fig. 1*C*). Concomitant with these morphological changes, the expression of ppGalNAc-T13 increased first to a peak on day 7 and then decreased on day 9 (Fig. 1, *D* and *E*). Double immunostaining of the primary neuronal cultures on day 7, intriguingly, showed that ppGalNAc-T13 was predominantly co-expressed with the neural stem cell marker Nestin as well as the pan-neuronal marker β-III-tubulin but not with the astrocyte marker GFAP (Fig. 1*F*), suggesting a cell type-specific distribution of ppGalNAc-T13 in neural stem cells and neurons.

The P19 embryonal carcinoma cell line is a well established model system for analyzing the factors that regulate neuronal differentiation (29–31). P19 cells could differentiate into neurons as well as monolayer non-neuronal cells with astroglia morphology after induction with retinoic acid (ATRA) (29, 32). Therefore, we also checked the expression of ppGalNAc-T13 in this system. Fig. 2*A* shows a schematic of ATRA-induced neuronal differentiation of P19 cells. It comprises two major stages: neural induction and neuronal differentiation. During neural induction, pluripotent P19 cells are allowed to aggregate and form embryonic bodies with increased expression of the neural stem cell marker Nestin (31). When neuronal differentiation occurs, most of the neural stem cells begin to differentiate into neurons, accompanied by an increased expression of a pan-neuronal marker, β-III-tubulin (30, 31), whereas a small number of them could also differentiate into monolayer non-neuronal cells with astroglia morphology (29, 32). As shown in Fig. 2*B*, these characteristic changes in cell morphology during neuronal differentiation were clearly observed in our system, and

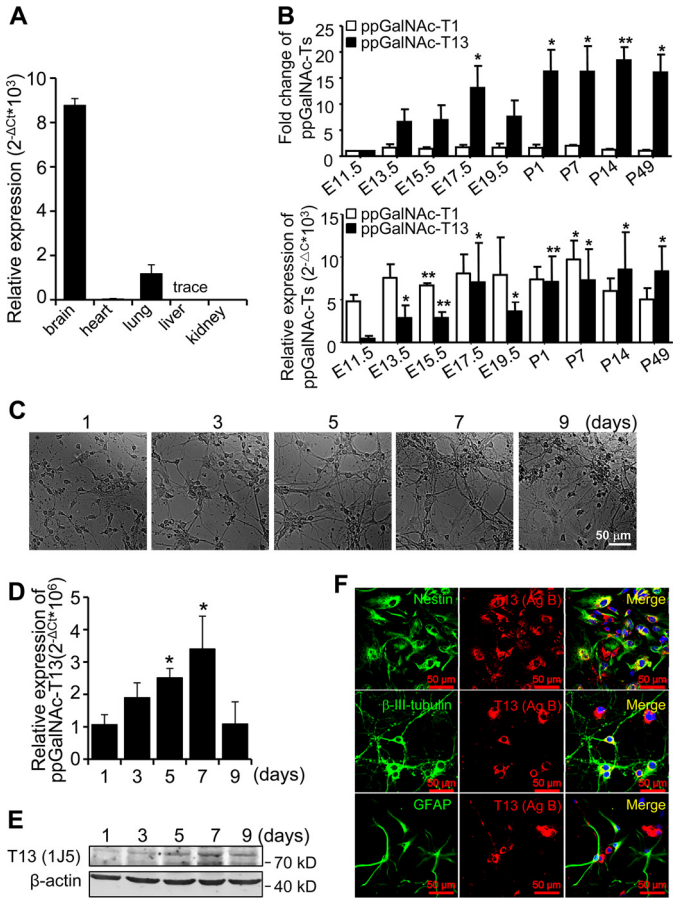

FIGURE 1. **The expression of ppGalNAc-T13 is up-regulated during mouse brain development as well as neuronal differentiation of mouse cortical neural precursor cells.** *A* and *B*, qRT-PCR using total RNA extracted from different tissues of P1 mice (*A*) or brains at the different stages of development (*B*) was carried out to examine the expression levels of *ppGalNAc-T13* and *ppGalNAc-T1* in mice. *Gapdh* was used as an internal control. The -fold changes of *ppGalNAc-T13* and *ppGalNAc-T1* expression were calculated based on the results of qRT-PCR (compared with E11.5; (E11.5–19.5) and postnatal days 1 (P1) to P49). To confirm the expression pattern of *ppGalNAc-T13* during neuronal differentiation, primary cortical neural precursor cells from the mouse brain at E17.5 were isolated and cultured as described under "Experimental Procedures." *C*, representative images of primary neuronal cultures on days 1, 3, 5, 7, and 9 were captured. *D*, qRT-PCR using total RNA extracted from these cells was performed to analyze the mRNA levels of *ppGalNAc-T13*. *Gapdh* was used as an internal control. *E*, the corresponding protein levels of ppGalNAc-T13 were examined by Western blotting analysis. β-Actin was used as a loading control. *F*, to determine the cellular distribution of ppGalNAc-T13 in the brain, double immunostaining of primary neuronal cultures on day 7 was performed using anti-ppGalNAc-T13 antibody (*red*) paired with antibodies (*green*) against Nestin (neural stem cell marker), β-III-tubulin (pan-neuronal marker), or GFAP (astrocyte marker). The quantitative data were obtained from three independent experiments. *Error bars* indicate standard deviation. The *p* values were calculated using two-tailed unpaired *t* test. *, $p < 0.05$; **, $p < 0.01$ (*versus* E11.5 or day 1).

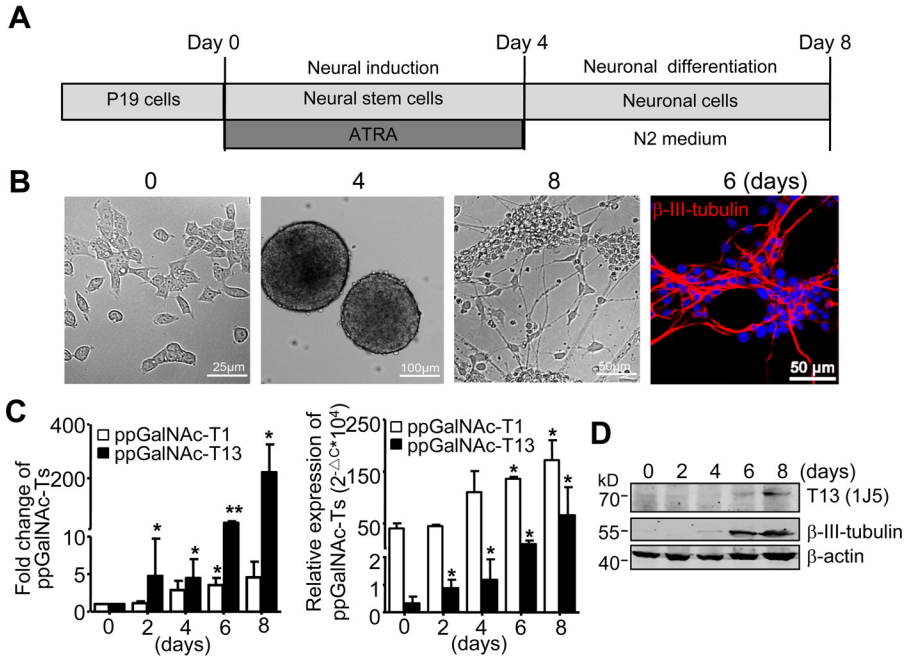

FIGURE 2. **ppGalNAc-T13 expression is increased during neuronal differentiation of P19 cells.** *A*, schematic of neuronal differentiation of P19 cells. P19 cells were initially induced by 1 μM ATRA to allow the formation of embryonic body-like structures. After 4 days, spherical embryoid bodies were dissociated and replated into DMEM/F12 1:1 medium containing 1% N2 to promote neurite formation and neuronal interaction. *B*, representative images were captured during neuronal differentiation of P19 cells. To confirm the successful establishment of this model, cells on day 6 were immunostained with anti-β-III-tubulin antibody (*red*). The nuclei were visualized by staining with DAPI (*blue*). *C*, the mRNA levels of *ppGalNAc-T13* and *ppGalNAc-T1* at the indicated times during neuronal differentiation of P19 cells were detected by qRT-PCR. *Gapdh* was used as an internal control. The -fold changes were calculated based on the results of qRT-PCR (compared with day 0). *D*, the corresponding protein levels of ppGalNAc-T13 and β-III-tubulin were analyzed by Western blotting analysis. β-Actin was used as a loading control. The quantitative data were obtained from three independent experiments. *Error bars* indicate standard deviation. The *p* values were calculated using two-tailed unpaired *t* test. *, $p < 0.05$; **, $p < 0.01$ (*versus* day 0).

our immunostaining assay revealed a high expression of β-III-tubulin in the cells on day 6. Meanwhile, Western blotting analysis showed that β-III-tubulin expression was significantly up-regulated during the stage of neuronal differentiation (Fig. 2*D*). These results suggest the successful establishment of the neuronal differentiation model in this study. Based on analyses by qRT-PCR and Western blotting (Fig. 2, *C* and *D*), we found that the expression of *ppGalNAc-T13* was markedly increased during neuronal differentiation of P19 cells, whereas *ppGalNAc-T1* was persistently expressed at a high level and had a slight change. These results are consistent with the observation *in vivo*. Taken together, our results clearly demonstrate that, unlike the small change of ppGalNAc-T1, ppGalNAc-T13 expression is dramatically up-regulated during neurogenesis, indicating a potential role of ppGalNAc-T13 in this process.

Knockout of ppGalNAc-T13 Inhibits Neuronal Differentiation of P19 Cells—To directly assess the functional contributions of ppGalNAc-T13 in neuronal differentiation, we knocked out the endogenous *ppGalNAc-T13* of P19 cells by CRISPR/Cas9 genome editing technology. Two clones (C4 and C13) with different frameshift mutations in *ppGalNAc-T13* gene were obtained and verified by DNA sequencing and Western blotting analysis (Fig. 3, *A* and *B*). Upon treatment with ATRA, both of the clones showed a significant decrease in the aggregate size of neural stem cells on day 4 compared with wild-type P19 cells (Fig. 3, *C* and *D*). In detail, in contrast to control cells whose aggregate diameters mostly ranged from 70–110 μm, we found that most of the ppGalNAc-T13 knockout aggregates had a diameter of 50–90 μm (Fig. 3*E*), suggesting a critical role of ppGalNAc-T13 in neural induction. Consistent with these morphological changes, a clear reduction in the expression of *Nestin* was observed after the loss of ppGalNAc-T13 (Fig. 3*F*). In addition to the effect on neural induction, ppGalNAc-T13 knockout also led to an inhibition of neuronal differentiation. This was evidenced not only by the increased monolayer non-neuronal cells during the neuronal differentiation stage (Fig. 3, *G* and *H*) but also by the reduced number of β-III-tubulin-positive cells (Fig. 3, *I* and *J*) as well as β-III-tubulin expression in whole cell lysates (Fig. 3*B*). Taken together, these results demonstrate that ppGalNAc-T13 is important for both neural induction and neuronal differentiation of P19 cells.

The Regulatory Effects of ppGalNAc-T13 on Neuronal Differentiation Are Mediated by PDPN, a Typical Mucin-type O-glycoprotein—The question arises of how ppGalNAc-T13 functions in neuronal differentiation. The marked enhancement of ppGalNAc-T13 expression was reminiscent of a typical mucin-type *O*-glycoprotein PDPN, which has also been reported to increase dramatically during the neuronal differentiation of P19 cells (33, 34). Consistently, such an increase was also observed in our neuronal differentiation model of both primary cortical neural precursor cells and P19 cells by Western blotting analysis (Fig. 4, *A* and *B*). These observations prompted us to ask whether ppGalNAc-T13 affects neuronal differentiation via PDPN. To test this, we first checked the effects of ppGalNAc-T13 on PDPN expression. Interestingly, knockout of ppGalNAc-T13 resulted in a clear decrease in PDPN expression (Fig. 4*C*). To further confirm the hypothesis above, we next knocked down *Pdpn* by RNA interference tech-

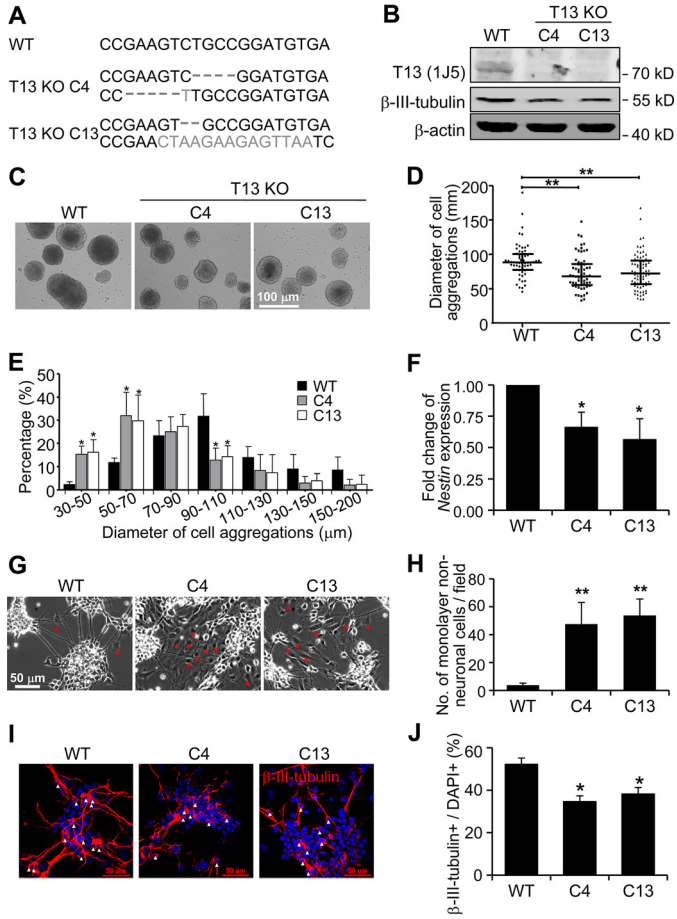

FIGURE 3. **Knockout of ppGalNAc-T13 in P19 cells inhibits not only neural induction but also neuronal differentiation.** *A*, sequences of the *ppGalNAc-T13* gene in WT and ppGalNAc-T13 mutant cells. *B*, to confirm the knockout of ppGalNAc-T13, neuronal differentiation of wild-type P19 cells and two ppGalNAc-T13 knockout clones was induced, and the expression levels of ppGalNAc-T13 and β-III-tubulin on day 8 were examined by Western blotting analysis. β-Actin was used as a loading control. *C*, to check the effect of ppGalNAc-T13 knockout on neural induction, representative images of aggregated cells on day 4 were captured. *D*, their diameter was statistically analyzed and is presented by median/scatter dot plot. *E*, the percentage of cell aggregates with different diameters (from eight fields containing at least 50 aggregates) was statistically analyzed. *F*, the relative expression levels of *Nestin* were detected by qRT-PCR. *Gapdh* was used as an internal control. *G*, to further check the effect of ppGalNAc-T13 knockout on neuronal differentiation, representative images of the indicated cells on day 8 were captured. Typical monolayer non-neuronal cells are indicated by *red triangles*. *H*, the number of these cells from five different fields was statistically analyzed. *I*, immunostaining of differentiated P19 cells on day 6 was carried out with antibody against β-III-tubulin (*red*). The nuclei were visualized by staining with DAPI (*blue*). β-III-tubulin-positive cells are indicated by *white triangles*. *J*, the percentages of β-III-tubulin-positive cells were determined by the number of β-III-tubulin-positive cells within more than 1000 cells and 10 fields. The quantitative data were obtained from three independent experiments. *Error bars* indicate standard deviation. The *p* values were calculated using two-tailed unpaired *t* test. *, $p < 0.05$; **, $p < 0.01$ (*versus* WT).

nology in P19 cells and examined the effects on neuronal differentiation. Fig. 4*D* shows efficient shRNA-mediated silencing of *Pdpn*. Like ppGalNAc-T13 knockout, knockdown of PDPN also reduced the aggregate size of neural stem cells (Fig. 4, *E* and *F*). The majority of cell aggregates formed by control cells had diameters of 70–110 μm, whereas the diameters of cell aggregates formed by PDPN knockdown P19 cells mainly ranged from 50–90 μm (Fig. 4*G*). In addition, knockdown of PDPN also inhibited neuronal differentiation, as seen not only by increased monolayer non-neuronal cells after silencing *Pdpn* (Fig. 4, *H* and *I*) but also by a significant decrease in the number of β-III-tubulin-positive cells (Fig. 4, *J* and *K*) and the expression of β-III-tubulin in the whole cell lysates (Fig. 4*D*). These results suggest that PDPN is also critical for the neuronal differentiation of P19 cells. So it is reasonable to conclude that PDPN, at least in part, mediates the effects of ppGalNAc-T13 on neuronal differentiation.

PDPN Acts as a Substrate of ppGalNAc-T13 and ppGalNAc-T1, and Some Sites on PDPN Could Be Glycosylated Only by ppGalNAc-T13—Different ppGalNAc-Ts display distinct substrate specificities (35). To determine whether ppGalNAc-T13 is responsible for the *O*-glycosylation of PDPN, an *in vitro* enzymatic activity assay was carried out using peptide fragments of PDPN with potential *O*-glycosylation sites (Fig. 5*A*). As shown in Fig. 5*B*, all five peptides could be glycosylated by the recombinant ppGalNAc-T13, indicating that PDPN serves as a substrate of ppGalNAc-T13. In addition to ppGalNAc-T13, we also checked the activity of ppGalNAc-T1 and ppGalNAc-T2. In contrast to the weak activity of ppGalNAc-T2, ppGalNAc-T1 also had high activities to PDPN peptides like ppGalNAc-T13. However, notably, on PDPN peptide S4, we found a specific product peak (P4) of ppGalNAc-T13 that was not produced by ppGalNAc-T1 (Fig. 5, *B* and *C*). MALDI-TOF mass analysis showed that, like the common product P3, this ppGalNAc-T13-specific product also contained two GalNAc moieties (Fig. 5*D*). These results demonstrate that both of ppGalNAc-T13 and ppGalNAc-T1 could glycosylate PDPN but that there exist some sites on PDPN that could be specifically glycosylated by ppGalNAc-T13.

O-glycosylation of PDPN Is Important for Its Stability—Next, to explore the mechanisms by which ppGalNAc-T13 regulates the expression of PDPN, we examined the transcriptional level of *Pdpn* in ppGalNAc-T13 knockout clones. Intriguingly, no big change was observed after ppGalNAc-T13 knockout (Fig. 6*A*), suggesting that ppGalNAc-T13 may regulate the expression of PDPN at a posttranscriptional level. Consistent with this hypothesis, there was little difference in the transcription of *Pdpn* during the neuronal differentiation of either primary cortical neural precursor cells or P19 cells (Fig. 6*A*), although its protein level increased dramatically as described above. Given the accumulating evidence for the importance of *O*-glycosylation in protein stability (36–39), we then investigated the effects of *O*-glycosylation on the stability of PDPN using two CHO cell lines CHO-K1 and CHO-ldlD. CHO-ldlD is an *O*-glycosylation-deficient cell line because of the lack of the epimerase that converts UDP-Glc/GlcNAc to UDP-Gal/GalNAc (40). Therefore, in contrast to CHO-K1 cells, where the majority of the FLAG-tagged PDPN protein overexpressed was hyperglycosylated, the recombinant PDPN in CHO-ldlD cells was exclusively underglycosylated (Fig. 6, *B* and *C*). To compare the relative half-life of PDPN in these cells, translation was arrested by treatment with 100 μg/ml cycloheximide (CHX). At various times after CHX addition, protein was extracted, and total PDPN was semiquantified by Western blotting analysis. As seen in Fig. 6*B*, a significant amount of hyperglycosylated PDPN was still detectable after 16 h ($t_{1/2}$, ~24 h) in CHO-K1 cells. In contrast, most of the underglycosylated PDPN was

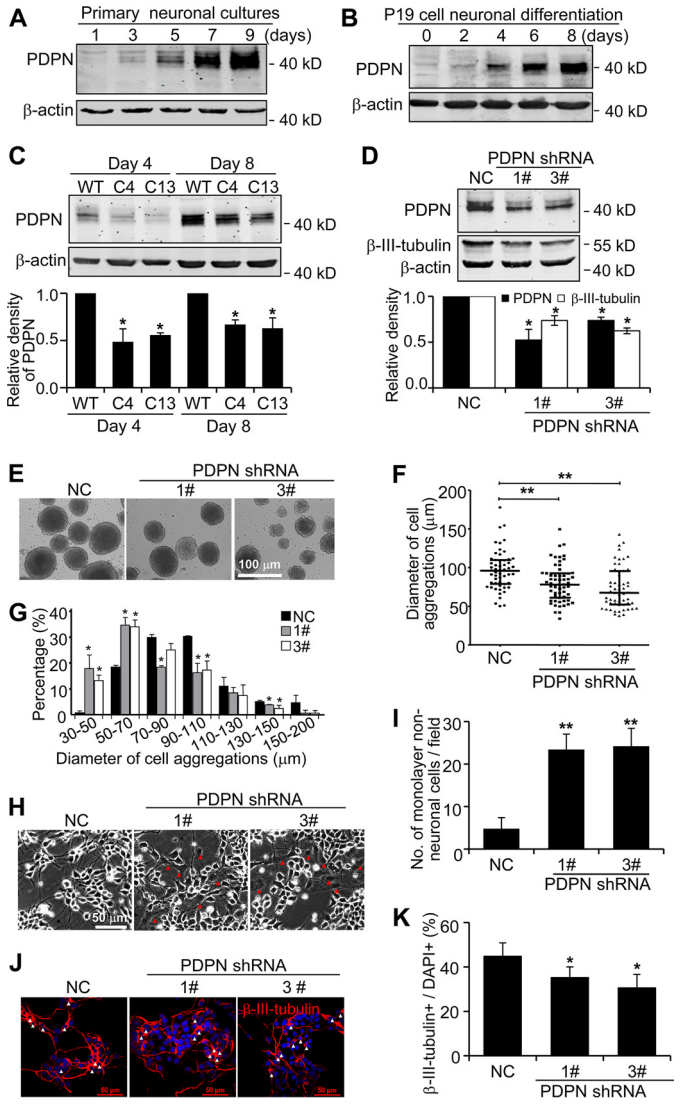

FIGURE 4. **The classical mucin-type *O*-glycoprotein PDPN is involved in mediating the regulatory effects of ppGalNAc-T13 in neuronal differentiation.** *A* and *B*, cell lysates prepared from primary neuronal cultures (*A*) and P19 cells (*B*) at the indicated times of neuronal differentiation were immunoblotted with anti-PDPN antibody. *C*, to determine the effect of ppGalNAc-T13 knockout on PDPN expression, the protein levels of PDPN in wild-type and ppGalNAc-T13 knockout P19 cells at the indicated times were examined by Western blotting analysis. β-Actin was used as a loading control. To check whether PDPN was also involved in neuronal differentiation, scramble (NC) or *Pdpn*-targeted shRNA (*1#*, *3#*) was transfected into P19 cells. *D*, after 6–12 h, the cells were induced to neuronal differentiation by ATRA, and cell lysates from the indicated cells on day 8 were immunoblotted with anti-PDPN and β-III-tubulin antibodies to confirm the knockdown efficiency of PDPN. β-Actin was used as a loading control. The density of the band was semiquantified by QuantityOne software. *E*, to check the effect of PDPN knockdown on neural induction, representative images of the cell aggregation of shRNA-transfected P19 cells on day 4 were captured. *F*, their diameter was statistically analyzed and is presented by median/scatter dot plot. *G*, the percentage of cell aggregates with different diameters (using eight fields containing at least 50 aggregates) was statistically analyzed. *H*, to check the effect of PDPN knockdown on neuronal differentiation, representative images of the neuronal morphologies of the indicated cells on day 8 were captured. Typical monolayer non-neuronal cells are indicated by *red triangles*. *I*, the number of these cells from five different fields was statistically analyzed. *J*, immunostaining of differentiated P19 cells on day 6 was carried out with the antibody against β-III-tubulin (*red*). The nuclei were visualized by staining with DAPI (*blue*). β-III-tubulin-positive cells are indicated by *white triangles*. *K*, the percentages of β-III-tubulin-positive cells were determined by the number of β-III-tubulin-positive cells within more than 1000 cells and 10 fields. The quantitative data were obtained from three independent experiments. *Error bars* indicate standard deviation. The *p* values were calculated using two-tailed unpaired *t* test. *, $p < 0.05$; **, $p < 0.01$ (*versus* NC).

already degraded after 12 h ($t_{1/2}$, ~14 h) in the CHO-ldlD cells (Fig. 6, *C*, *I*, and *J*). Addition of exogenous GalNAc and Gal into the culture medium of CHO-ldlD cells clearly enhanced the level of hyperglycosylated PDPN (Fig. 6*D*) and prevented protein decay ($t_{1/2}$, ~18 h) (Fig. 6, *I* and *J*). These results clearly demonstrate that *O*-glycosylation is important for the stabilization of PDPN. Consistently, concomitant expression of either ppGalNAc-T13 or ppGalNAc-T1 in CHO-K1 or CHO-ldlD cells led to a further increase in the expression of hyperglycosylated PDPN (Fig. 6, *E–J*) as well as its half-life, suggesting that ppGalNAc-T13- or ppGalNAc-T1-mediated *O*-glycosylation could facilitate the stabilization of PDPN. These data suggest that *O*-glycosylation on PDPN is critical for its stability.

Overexpression of ppGalNAc-T13, but Not ppGalNAc-T1, Rescues the Neuronal Differentiation Defect of ppGalNAc-T13-deficient P19 Cells—Although knockout of *ppGalNAc-T13* using the CRISPR-Cas9 system inhibited neuronal differentiation of P19 cells, the influence could be due to potential off-target effects of the designed sequence. To rule out this possibility, we overexpressed ppGalNAc-T13 in ppGalNAc-T13 knockout P19 cells. The expression level was verified by Western blotting analysis (Fig. 7*E*). Restoration of ppGalNAc-T13 expression rescued the defects in neuronal differentiation to a large extent, as shown by the significant decrease in monolayer non-neuronal cells (Fig. 7, *A* and *B*) and the increase in the number of β-III-tubulin-positive cells (Fig. 7, *C* and *D*) compared with ppGalNAc-T13 knockout P19 cells. Also, PDPN in the ppGalNAc-T13-overexpressing cells was up-regulated to a level comparable with that seen in wild-type P19 cells despite the small difference in its transcription (Fig. 7, *E* and *F*). These results further corroborated that ppGalNAc-T13 may contribute to neuronal differentiation by glycosylating and stabilizing PDPN. Given the fact that ppGalNAc-T13 shows high homology to the ubiquitous ppGalNAc-T1 and that ppGalNAc-T1 also facilitated the stabilization of PDPN in CHO cells (28), we asked whether ppGalNAc-T1 could complement the function of ppGalNAc-T13 in neurogenesis. To test this idea, we overexpressed ppGalNAc-T1 in ppGalNAc-T13 knockout cells and replicated the experiments above. As shown in Fig. 7, *A–E*, overexpression of ppGalNAc-T1 rescued the expression of PDPN but had little effects on the emergence of β-III-tubulin-positive cells and monolayer non-neuronal cells, indicating a distinct role of ppGalNAc-T13 in neuronal differentiation. Taken together, our results demonstrate that ppGalNAc-T13 promotes neurogenesis at least in part through glycosylating and stabilizing the mucin-type *O*-glycoprotein PDPN.

Discussion

In contrast to the growing evidence for the importance of *O*-glycosylation in organ development and various diseases (12, 17, 23, 41), there is a particular dearth of information regarding its roles in neural development. Previously, our group found that ppGalNAc-T13 is restrictively expressed at a high level in the brain (28). This raised the question of whether it functions

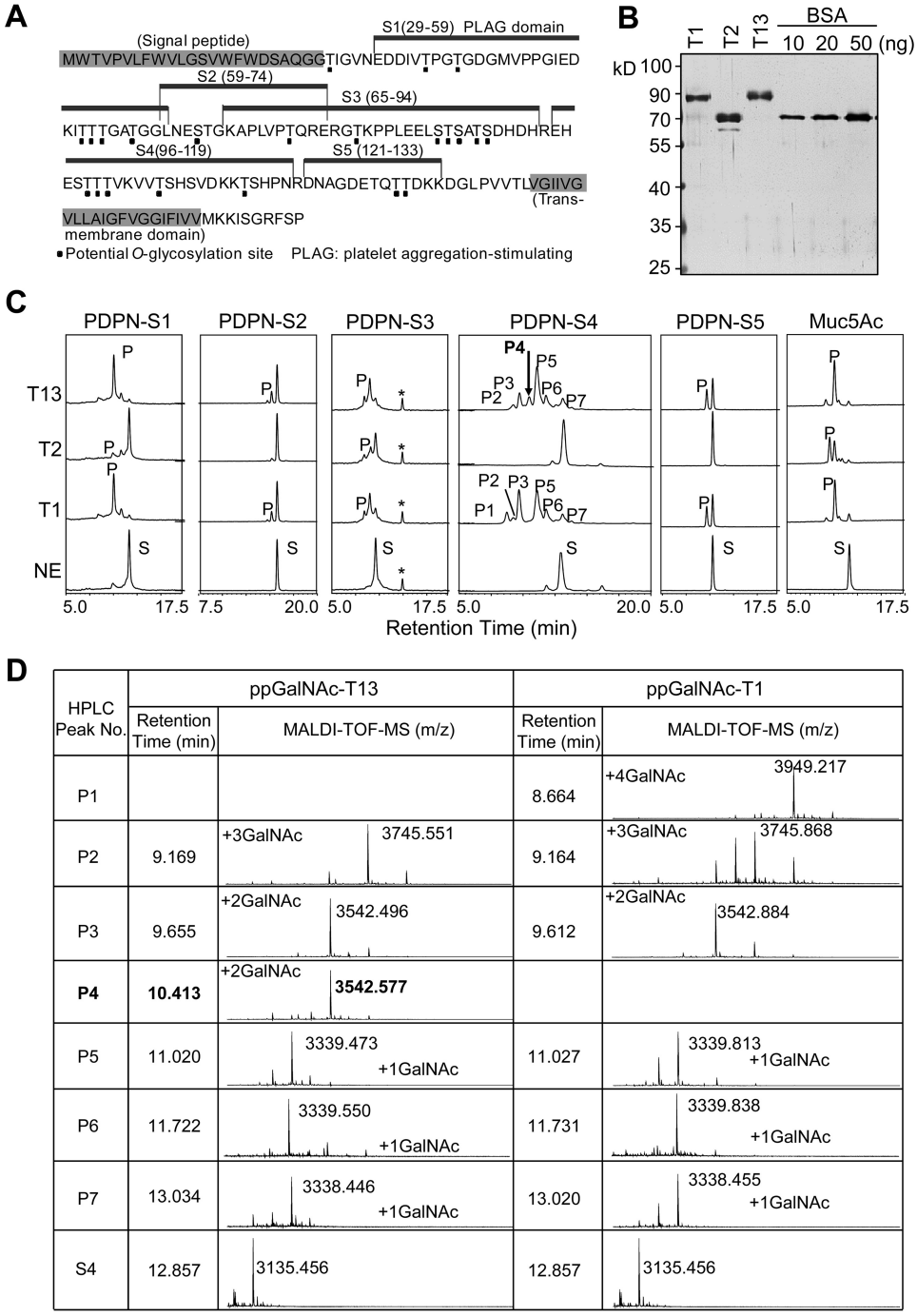

HPLC Peak No.	ppGalNAc-T13 Retention Time (min)	ppGalNAc-T13 MALDI-TOF-MS (m/z)	ppGalNAc-T1 Retention Time (min)	ppGalNAc-T1 MALDI-TOF-MS (m/z)
P1			8.664	+4GalNAc 3949.217
P2	9.169	+3GalNAc 3745.551	9.164	+3GalNAc 3745.868
P3	9.655	+2GalNAc 3542.496	9.612	+2GalNAc 3542.884
P4	**10.413**	+2GalNAc **3542.577**		
P5	11.020	3339.473 +1GalNAc	11.027	3339.813 +1GalNAc
P6	11.722	3339.550 +1GalNAc	11.731	3339.838 +1GalNAc
P7	13.034	3338.446 +1GalNAc	13.020	3338.455 +1GalNAc
S4	12.857	3135.456	12.857	3135.456

FIGURE 5. **PDPN is a substrate of ppGalNAc-T13 and ppGalNAc-T1, whereas some sites on PDPN could be glycosylated only by ppGalNAc-T13.** *A*, to test whether ppGalNAc-T13 could glycosylate PDPN, an *in vitro* enzymatic activity assay was performed using the recombinant ppGalNAc-Ts and five peptide fragments of PDPN with potential *O*-GalNAc glycosylation sites. The potential glycosylation sites were predicted with NetOGlyc 4.0 and are indicated by *black dots*. *B*, the purity of the recombinant ppGalNAc-Ts was checked by silver staining analysis. BSA served as the standard for quantization. *C*, the ability of ppGalNAc-T1, T2, and T13 to glycosylate five PDPN peptides was determined by reverse-phase HPLC. Muc5Ac served as the positive control. The peaks of glycosylated peptides were shifted to the left. *S*, substrates; *P*, products. The *asterisks* indicates a contaminant. The *black arrow* indicates the specific product peak of ppGalNAc-T13 (P4 of PDPN-S4). *D*, to clarify the difference in substrate specificities between ppGalNAc-T1 and T13, this ppGalNAc-T13-specific peak, together with other common peaks derived from ppGalNAc-T13- or ppGalNAc-T1-treated PDPN-S4, was isolated and subjected to MALDI-TOF mass analysis.

in brain development. In this study, we demonstrate that high expression of ppGalNAc-T13 contributes to neuronal differentiation by glycosylating and stabilizing the mucin-type *O*-glycoprotein PDPN.

CNS development is a complex process that is precisely regulated by a large set of transcription factors (42–44). Our results showed that the expression of ppGalNAc-T13 was markedly up-regulated during neurogenesis in the mouse embryonic brain and sustained a high level at the postnatal stage. This could be partly mediated by PAX7, a neuron-specific transcription factor that also occurs from early development and persists in restricted regions, including neurons, throughout adulthood (45), because PAX7 has been reportedly involved in the regulation of ppGalNAc-T13 transcription (46),

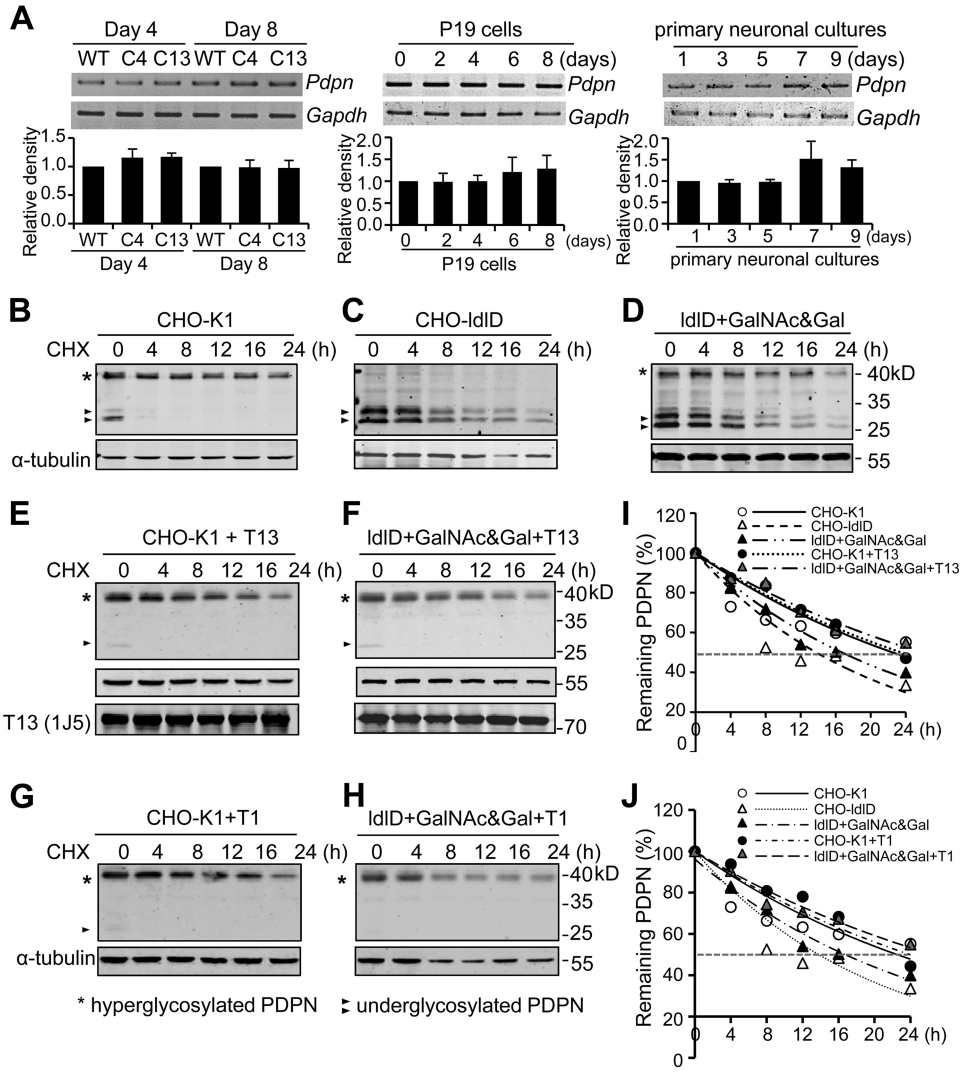

FIGURE 6. **The *O*-glycosylation modification on PDPN is important for its stability.** *A*, to confirm whether ppGalNAc-T13 regulates PDPN at the transcriptional level, the mRNA levels of *Pdpn* were examined by RT-PCR using total RNA extracted from wild-type and ppGalNAc-T13 knockout P19 cells at the indicated times. Also, RT-PCR was carried out to check the transcription of *Pdpn* during the neuronal differentiation of P19 cells and primary cortical neural precursor cells. *Gapdh* was used as a loading control. The density of the band was semiquantified by QuantityOne software. *B* and *C*, to examine the influence of *O*-glycosylation modification on PDPN stability, CHO-K1 (*B*) and CHO-ldlD (*C*) cells were transfected with PDPN-FLAG, and translation was arrested by treatment with 100 μg/ml CHX. At various times after CHX addition, protein was extracted, and then total PDPN was semiquantified by Western blotting analysis with anti-FLAG and anti-α-tubulin antibodies. *D–H*, to further confirm the effect of *O*-glycosylation modification on the half-life of PDPN, CHO-K1 or CHO-ldlD cells with/without the co-transfection of ppGalNAc-T13 or ppGalNAc-T1 were cultured with the addition of 200 μM GalNAc and Gal in their medium. The experiments above were replicated. *Asterisks* indicate hyperglycosylated PDPN, and *black triangles* indicate underglycosylated PDPN. *I* and *J*, the relative expression of total PDPN at the indicated time points was calculated by normalization of the intensities of PDPN bands with that of α-tubulin and fitted to the exponential curves. The relative half-life of PDPN in different cells is indicated by the *gray dashed line*.

and overexpression of PAX7 is capable of promoting the neuronal differentiation of P19 cells (47). However, during brain development, a momentary decrease in ppGalNAc-T13 expression was observed at E19.5. In general, this time point in mouse brain development corresponds to the period of gliogenesis, particularly the generation of astrocytes (48). Given our immunostaining result that ppGalNAc-T13 was specifically expressed in neural stem cells and neurons but not in astrocytes, it is reasonable to attribute the reduction at E19.5 to the enhanced proportion of astrocytes in the mouse brain we isolated. Consistent with this hypothesis, a similar decrease in ppGalNAc-T13 expression was observed, accompanied by a dramatic increase in expression of the astrocyte marker *Gfap* (data not shown) on day 9 of the primary neuronal cultures. In contrast, ppGalNAc-T13 expression was consistently up-regulated during the neuronal differentiation of P19 cells, where astrocytes were rarely generated (49, 50). Collectively, these results indicate that ppGalNAc-T13 could serve as a marker for neural stem cells and neurons.

PDPN is a classical mucin-type glycoprotein that has been not only well known for its functions in the activation of platelet aggregation and maintenance of the normal development of lymphatic vessels (51) but associated with the progression of multiple types of carcinomas (52, 53). Our results demonstrate for the first time that PDPN is also involved in neuronal differentiation, as knockdown of PDPN in P19 cells resulted in a significant inhibition of neuronal differentiation-related morphological and molecular changes. Considering also that

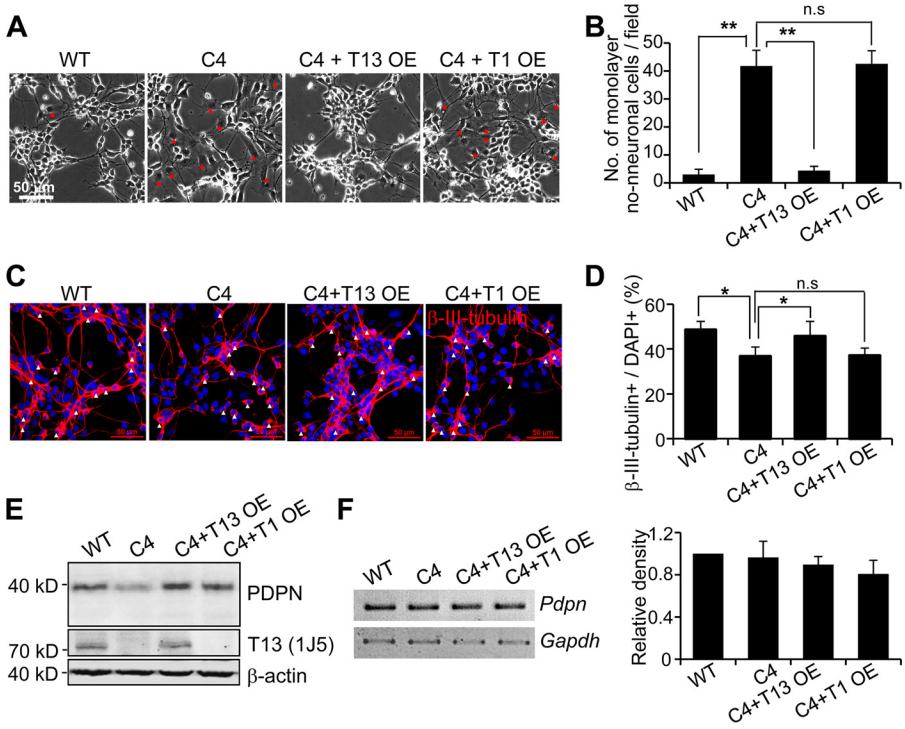

FIGURE 7. **Forced expression of ppGalNAc-T13, but not ppGalNAc-T1, rescues the defects in neuronal differentiation of ppGalNAc-T13 knockout P19 cells.** Neuronal differentiation of ppGalNAc-T13 knockout cells (C4) overexpressing ppGalNAc-T13 or ppGalNAc-T1 was induced as described under "Experimental Procedures." *A*, representative images of the neuronal morphologies of the indicated cells on day 8 were captured. Typical monolayer non-neuronal cells are indicated by *red triangles*. *B*, the number of these cells from five different fields was statistically analyzed. *C*, immunostaining of differentiated P19 cells on day 6 was carried out with the antibody against β-III-tubulin (*red*). The nuclei were visualized by staining with DAPI (*blue*). β-III-tubulin-positive cells are indicated by *white triangles*. *D*, the percentages of β-III-tubulin-positive cells were determined by the number of β-III-tubulin-positive cells within more than 1000 cells and 10 fields. *E*, to check the protein level of PDPN after overexpression of ppGalNAc-T13 or ppGalNAc-T1 in ppGalNAc-T13 knockout cells, cell lysates from the indicated cells on day 8 were subjected to SDS-PAGE and immunoblotted with anti-PDPN and anti-ppGalNAc-T13 antibodies. β-Actin was used as a loading control. *F*, RT-PCR using total RNA from the indicated cells was carried out to examine the mRNA levels of *Pdpn*. *Gapdh* was used as a loading control. The density of the band was semiquantified by QuantityOne software. The quantitative data were obtained from three independent experiments. *Error bars* indicate standard deviation. The *p* values were calculated using two-tailed unpaired *t* test. *, $p < 0.05$; **, $p < 0.01$ (*versus* WT).

ppGalNAc-T13 deficiency clearly reduced PDPN expression in a posttranscriptional manner and that increasing the *O*-glycosylation level of PDPN by forced expression of ppGalNAc-T13 led to an enhancement in the half-life of PDPN, it is reasonable to conclude that ppGalNAc-T13 promotes neurogenesis at least in part by conferring stability to PDPN. However, paradoxically, a recent study reported that lack of core 1 *O*-glycosylation does not affect intracellular trafficking or protein turnover of PDPN (54). One possible interpretation for these differences is that the stability of PDPN depends on whether the important site is glycosylated instead of how complex the glycan structure is. Despite clear evidence for the involvement of ppGalNAc-T13 in PDPN stability, we still could not rule out the possibility that ppGalNAc-T13 may also contribute to neuronal differentiation by facilitating the interaction between PDPN and its receptors because the *O*-glycosylation on the platelet aggregation-stimulating domain of PDPN has been reported to be important for the interaction with its receptor CLEC-2 (55–57). Consistent with this hypothesis, our *in vitro* enzymatic activity assay showed that ppGalNAc-T13 had a high preference for the peptide substrate (S1) covering the platelet aggregation-stimulating domain of PDPN. It should be noted that, in addition to S1, the peptide fragments S3 and S4 were also liable to be glycosylated by ppGalNAc-T13. Considering its high preference for the triple T antigen nouvelle (Tn) epitope site (28), such substrate specificities of ppGalNAc-T13 are conceivably due to the existence of consecutive Ser/Thr residues in these three peptide fragments, and whether these triple T antigen nouvelle (Tn) epitope sites on PDPN are involved in the interaction with its ligands in neurogenesis remains to be determined.

Although ppGalNAc-T1 shares high homology with ppGalNAc-T13, our data demonstrate a distinctive role of ppGalNAc-T13 in neurogenesis because overexpression of ppGalNAc-T13, but not ppGalNAc-T1, rescued the defects in neuronal differentiation of ppGalNAc-T13 knockout P19 cells. However, the expression of PDPN was restored in either ppGalNAc-T13 or ppGalNAc-T1-overexpressing cells. Considering also our result that ppGalNAc-T1-mediated *O*-glycosylation facilitated the stabilization of PDPN, it is conceivable that the *O*-glycosylation level of PDPN is important for its stability, whether it is catalyzed by ppGalNAc-T13 or not. But why did the restored PDPN after ppGalNAc-T1 overexpression fail to rescue the defects in the differentiation into β-III-tubulin positive cells? One possibility is that there is/are glycosylation site(s) on PDPN that is/are important for its functional contribution in neurogenesis and that these site(s) could be glycosylated by ppGalNAc-T13 but not ppGalNAc-T1, as several groups, including us, have revealed a significant difference in the preference for glycopeptides between ppGalNAc-T13 and ppGalNAc-T1 (28, 58,

59). In agreement with this, our *in vitro* study using different peptide fragments of PDPN as substrates revealed a specific product peak of ppGalNAc-T13 on peptide S4, and this peak should not be random, as it was always specifically produced upon treatment with ppGalNAc-T13 when we changed the reaction time and enzyme amount. Furthermore, *O*-glycosylation prediction using the isoform-specific prediction tool ISOGlyP (60) showed that there are some potential sites on PDPN that could be glycosylated by ppGalNAc-T13 but not ppGalNAc-T1, which also supported our *in vitro* enzymatic activity results. In addition to the hypothesis above, it is also possible that there may exist some other proteins that mediate the functions of ppGalNAc-T13 in neurogenesis and that these proteins could be specifically glycosylated by ppGalNAc-T13. Besides PDPN, both sydecan-3 and syndecan-1 have been found to be the substrates of ppGalNAc-T13 (28, 61, 62), and sydecan-3 has been reportedly involved in axon guidance, neural migration, and neuronal plasticity (63, 64). Meanwhile, *O*-glycosylation modifications have also been observed on several neuron-specific transmembrane or matrix proteins such as p75 (neurotrophin receptor), amyloid precursor protein, neural cell adhesion molecule, and testicans (65–68), although little is known about their functions in neural development. Clearly, further study is needed to clarify the mechanisms of the distinct roles of ppGalNAc-T13 in neural differentiation.

In summary, this study convincingly demonstrates that ppGalNAc-T13 promotes neurogenesis at least in part by stabilizing PDPN, which not only gives a plausible explanation for the restrictive expression of ppGalNAc-T13 in the brain but also provides insights into the regulatory roles of *O*-glycosylation in mammalian neural development.

Experimental Procedures

Mice—Pregnant and postnatal C57BL/6J mice were purchased from the Model Animal Research Center of Nanjing University (Nanjing, China). The animal protocols were approved by the Institutional Animal Care and Use Committee of Shanghai Jiao Tong University.

Primary Cortical Neuronal Cultures—The neuronal differentiation of primary cortical neural precursor cells was performed as described previously (69). In brief, 17.5-day pregnant mice were sacrificed, and brain cortices from the fetuses were isolated. The cortices then were dispersed with 0.125% trypsin at 37 °C for 15 min, passed through screen mesh, and seeded at a density of 2.0×10^5 cells/cm^2 in DMEM/F12 1:1 supplemented with 10% FBS and 1% penicillin-streptomycin. After 4 h, the supernatants were removed, and cells were cultured in serum-free Neurobasal medium supplemented with 2% B27, 2 mM L-glutamine, and 1% penicillin-streptomycin. The regents used above were purchased from Invitrogen.

Cell Lines and Cell Culture—P19C6, a subclone of the mouse embryonal carcinoma P19 cell line, was provided by Dr. Naihe Jing (Institute of Biochemistry and Cell Biology, Chinese Academy of Sciences). P19 cells, CHO epitheloid cells (CHO-K1), and mutant cells (CHO-ldlD) (40) were maintained in DMEM/F12 1:1 medium containing 10% FBS and cultured under a humidified atmosphere containing 5% CO_2 at 37 °C.

Neuronal Differentiation of P19 Cells—Neuronal differentiation of P19 cells was induced by all-*trans*-retinoid acid (ATRA) as reported previously (29). In brief, cells were plated at 10^6 cells/bacteriological 10-cm Petri plate in α-minimal essential medium containing 10% FBS and 1 μM ATRA (Sigma) to allow the formation of embryoid body-like structures. After 4 days, spherical embryoid bodies were harvested, dissociated, and replated onto poly-L-lysine- and 1 μg/ml fibronectin-coated tissue culture dishes and cultured for another 4 days with DMEM/F12 1:1 medium containing 1% N2 (Invitrogen). The culture medium was changed every 2 days.

Establishment of the ppGalNAc-T13 Knockout P19 Cell Line—The single guide RNAs (forward, 5′-CACCCGCACTTAACCGAAGTCTGC-3′; reverse, 5′-AAACGCAGACTTCGGTTAAGTGCGC-3′) targeting exon 4 of the mouse *ppGalNAc-T13* gene were designed with an online tool and inserted into the pX330 plasmid. The constructed plasmids were then transfected into P19 cells using Lipofectamine 2000 transfection reagent (Invitrogen) according to the instructions of the manufacturer. After 24 h, the cells were suspended and diluted onto 96-well plates. Single colonies were selected, passaged, and genotyped. To verify the mutation in the *ppGalNAc-T13* gene, the genomic region around the target site was amplified by PCR using the primers 5′-TGCATAGAGAGTTTTCTTGTCTGA-3′ (forward) and 5′-AGAAAACAATTCATA TTTCTTAGCA-3′ (reverse) and subjected to digestion with T7E1 enzyme. To further confirm the indels, the products were cloned into the pGEM-T vector for sequencing.

RT-PCR for mRNA Expression Analysis—Total RNA was extracted from cultured cells or mouse tissues using Isol-RNA lysis reagent (Takara, Shiga, Japan), and 1 μg of total RNA was reverse-transcribed into cDNA using a PrimeScript RT reagent Kit with gDNA Eraser (Takara). The sequences of primers used for qRT-PCR analysis were as follows: *Gapdh* (5′-TTCAACAGCAACTCCCACTCTT-3′ and 5′-TGGTCCAGGGTTTCTTACTCC-3′), *ppGalNAc-T13* (5′-GCTGGCGAGAATAAAGGAAG-3′ and 5′-GGACAGGATACCATCGGAAA-3′), *ppGalNAc-T1* (5′-TGGTGATTGTTTTCCACAATGAG-3′ and 5′-TGGCGAGCGATTAATGACACT-3′), and *Nestin* (5′-GGTTCCCAAGGTCTCCAGAA-3′ and 5′-AAATGCCTGCTGGTCCTCTT-3′). qRT-PCR was performed (95 °C for 15 s, 60 °C for 1 min, 40 cycles) with Power SYBR Green Master Mix (Applied Biosystems, Warrington, UK) using the StepOne™ real-time PCR system (Applied Biosystems). The relative expression was calculated by the $2^{-\Delta Ct}$ formula and the $2^{-\Delta\Delta Ct}$ formula for the -fold changes. ΔCt was calculated by subtracting the Ct values of *Gapdh* from those of the *ppGalNAc-T*s. ΔΔCt was then calculated by subtracting ΔCt of the control sample. The sequences of primers used for semiquantitative RT-PCR were as follows: *Gapdh* (5′-TCCACCACCCTGTTGCTGTA-3′ and 5′-ACCACAGTCCATGCCATCAC-3′) and *Pdpn* (5′-TGCCAGTGTTGTTCTGGGTT-3′ and 5′-GGGCGAGAACCTTCCAGAAA-3′). The annealing temperatures and cycle numbers of *Gapdh* and *Pdpn* were 55 °C/25 cycles and 58 °C/30 cycles, respectively. The PCR products were analyzed by electrophoresis with 1.5% agarose gel.

RNA Interference—To knock down endogenous PDPN expression in P19 cells, the target sequences of *Pdpn* (5′-GCG-

TGAATGAAGATGATAT-3′ (1#) and 5′-GAGGGATCTTC-ATTGTTGT-3′ (3#)) were synthesized (Sangon, Shanghai, China) and inserted into the pmiRZip vector (System Bioscience). The sequence 5′-ACTACCGTTGTTATAGGTG-3′ was also inserted into the pmiRZip vector and used as the negative control (NC). P19 cells were transfected with scramble (NC) or PDPN-targeted shRNA plasmids using Lipofectamine 2000 transfection reagent (Invitrogen) according to the instructions of the manufacturer. After 6–12 h, the transfected cells were collected, counted, and induced by ATRA for neuronal differentiation as described above.

Overexpression of ppGalNAc-T13 and ppGalNAc-T1—To rescue the neuronal differentiation defects of ppGalNAc-T13 knockout cells, the pcDNA 3.1 plasmids inserted with full-length ppGalNAc-T13 or ppGalNAc-T1 were transfected into ppGalNAc-T13 knockout cells (C4) using Lipofectamine 2000 transfection reagent (Invitrogen) according to the instructions of the manufacturer. After 6–12 h, the transfected cells were collected, counted, and induced by ATRA for neuronal differentiation as described above.

Generation of Anti-ppGalNAc-T13 Antibodies—Sequence alignment between ppGalNAc-T1 and ppGalNAc-T13 indicates a unique fragment (RSLLPALRAVISRNQE) on the stem region of ppGalNAc-T13. The rabbit polyclonal antibody Ag B used for immunostaining analysis was constructed by the National Institute of Advanced Industrial Science and Technology (Japan) with the synthetic peptide SLLPALRAVISRNQ as an antigen. The mouse monoclonal antibody 1J5 against ppGalNAc-T13 was developed by Abmart Co. (Shanghai, China) using peptide fragment RSLLPALRAVISRNQE as an antigen. 1J5 is applicable for Western blotting analysis and has no cross-reactivity to other ppGalNAc-Ts (data not shown).

Western Blotting Analysis—Cells were washed with PBS and lysed in radioimmune precipitation assay buffer (150 mM NaCl, 50 mM Tris-HCl, 1% Nonidet P-40, and 0.1% SDS) containing protease inhibitor mixture (Roche, Indianapolis, IN). Protein concentrations were measured using the BCA assay (Thermo Fisher Scientific, Rockford, Illinois). Equal amounts of protein were subjected to SDS-PAGE, transferred to a nitrocellulose membrane, and probed with the appropriate antibodies. The blots were developed with the Odyssey infrared imaging system (LI-COR Biosciences, Lincoln, NE) and the following primary antibodies: anti-β-III-tubulin mouse monoclonal antibody (T8660, Sigma), anti-PDPN rabbit monoclonal antibody (clone EPR7073, Abcam), anti-ppGalNAc-T13 mouse monoclonal antibody (clone 1J5, hybridoma culture medium, Abmart), and anti-β-actin mouse monoclonal antibody (A2228, Sigma).

Immunofluorescence Staining—Cells on coverslips (Corning Glass) were fixed with 4% paraformaldehyde, permeabilized by methanol for 30 min at room temperature, and blocked with 5% BSA in PBS for 2 h. Then antibodies against Nestin (MAB353, Millipore), β-III-tubulin (T8660, Sigma), GFAP (3670, Cell Signaling Technology), or ppGalNAc-T13 (Ag B) were utilized, followed by appropriate Alexa Fluor 546- or 488-conjugated secondary antibodies (Invitrogen). Stained cells were mounted and visualized on a Nikon A1Si laser-scanning confocal microscope. Representative confocal images are shown in each figure.

Enzymatic Activity Assay of ppGalNAc-T13—GalNAc transferase activity was examined as described previously (11, 13). In brief, reactions were incubated at 37 °C and terminated by boiling for 5 min at 95 °C. PDPN peptides were designed according to the prediction of NetOGlyc 4.0. The amino acid sequence of Muc5Ac peptide is SAPTTSTTSAPTK-5.6FAM. All the peptides were synthesized by GL Biochem Ltd. (Shanghai, China). The secreted ppGalNAc-T1, T2, and T13 with the FLAG tag were obtained by transient transfection of HEK293 suspension cultures as described previously (28). For the determination of enzymatic activity, 20 ng of purified ppGalNAc-Ts were first incubated with 5′-carboxyfluorescein-labeled PDPN peptides at 37 °C for 9 h, and then the reaction mixtures were separated by reverse-phase HPLC (Shimadzu) using a C18 analytical column (COSMOSIL 5C18-AR-II, 4.6 × 250 mm).

MALDI-TOF-MS—Each peak of PDPN peptide S4 was collected by HPLC fractionation. 2,5-dihydroxybenzoic acid was used as the matrix. Mass spectra were acquired in positive ion mode using a MALDI-TOF mass spectrometer (UltrafleXtreme, Bruker Daltonics).

Determination of PDPN Half-life—CHO-K1 and CHO-ldlD cells were transfected with pcDNA-mPDPN-FLAG or pcDNA 3.1-ppGalNAc-T13/ppGalNAc-T1 plasmid using Lipofectamine 2000 transfection reagent (Invitrogen) for 24 h, followed by the treatment with 100 μg/ml CHX (Sigma). Cells were harvested at the indicated time points, and the whole lysates were subjected to SDS-PAGE and blotted with anti-FLAG (Abmart) or anti-α-tubulin (Proteintech, Wuhan, China) antibodies. To determine the half-life of PDPN, the total intensities of PDPN bands (hyper- or underglycosylated) were semiquantified using Quantity-One software (Bio-Rad) and normalized to the intensity of the α-tubulin band, the internal control.

Statistical Analysis—Statistical analysis was performed using two-tailed unpaired Student's *t* test with Microsoft Office Excel 2007 software.

Author Contributions—Y. Z. conceived the idea and supervised the study. Y. X., W. P., and A. S. performed the experiments. Y. X., J. L., and Y. Z. analyzed the experimental data. Y. X., J. L., and Y. Z. wrote and edited the manuscript. All authors analyzed the results and approved the final version of the manuscript.

Acknowledgments—We thank Dr. Hisashi Narimatsu and Dr. Takashi Sato for the anti-ppGalNAc-T13 antibody Ag B and helpful discussions. We also thank Dr. Naihe Jing for P19 cells and technical support for establishing the neuronal differentiation model, Dr. Lei Zhang for technical assistance, and Dr. Weijie Dong for performing the MALDI-TOF-MS analysis.

References

1. Livesey, F. J., and Cepko, C. L. (2001) Vertebrate neural cell-fate determination: lessons from the retina. *Nat. Rev. Neurosci.* **2,** 109–118
2. Sugimori, M., Nagao, M., Bertrand, N., Parras, C. M., Guillemot, F., and Nakafuku, M. (2007) Combinatorial actions of patterning and HLH transcription factors in the spatiotemporal control of neurogenesis and gliogenesis in the developing spinal cord. *Development* **134,** 1617–1629
3. Konopka, G., Bomar, J. M., Winden, K., Coppola, G., Jonsson, Z. O., Gao, F., Peng, S., Preuss, T. M., Wohlschlegel, J. A., and Geschwind, D. H. (2009) Human-specific transcriptional regulation of CNS development genes by FOXP2. *Nature* **462,** 213–217

4. Breen, K. C., Coughlan, C. M., and Hayes, F. D. (1998) The role of glycoproteins in neural development function, and disease. *Mol. Neurobiol.* **16,** 163–220
5. Ishii, A., Ikeda, T., Hitoshi, S., Fujimoto, I., Torii, T., Sakuma, K., Nakakita, S., Hase, S., and Ikenaka, K. (2007) Developmental changes in the expression of glycogenes and the content of *N*-glycans in the mouse cerebral cortex. *Glycobiology* **17,** 261–276
6. Ngamukote, S., Yanagisawa, M., Ariga, T., Ando, S., and Yu, R. K. (2007) Developmental changes of glycosphingolipids and expression of glycogenes in mouse brains. *J. Neurochem.* **103,** 2327–2341
7. Scott, H., and Panin, V. M. (2014) *N*-glycosylation in regulation of the nervous system. *Adv. Neurobiol.* **9,** 367–394
8. Dani, N., Zhu, H., and Broadie, K. (2014) Two protein *N*-acetylgalactosaminyl transferases regulate synaptic plasticity by activity-dependent regulation of integrin signaling. *J. Neurosci.* **34,** 13047–13065
9. Schjoldager, K. T., and Clausen, H. (2012) Site-specific protein *O*-glycosylation modulates proprotein processing: deciphering specific functions of the large polypeptide GalNAc-transferase gene family. *Biochim. Biophys. Acta* **1820,** 2079–2094
10. Zhang, L., Syed, Z. A., van Dijk Härd, I., Lim, J. M., Wells, L., and Ten Hagen, K. G. (2014) *O*-glycosylation regulates polarized secretion by modulating Tango1 stability. *Proc. Natl. Acad. Sci. U.S.A.* **111,** 7296–7301
11. Li, X., Wang, J., Li, W., Xu, Y., Shao, D., Xie, Y., Xie, W., Kubota, T., Narimatsu, H., and Zhang, Y. (2012) Characterization of ppGalNAc-T18, a member of the vertebrate-specific Y subfamily of UDP-*N*-acetyl-α-D-galactosamine:polypeptide *N*-acetylgalactosaminyltransferases. *Glycobiology* **22,** 602–615
12. Raman, J., Guan, Y., Perrine, C. L., Gerken, T. A., and Tabak, L. A. (2012) UDP-*N*-acetyl-α-D-galactosamine:polypeptide *N*-acetylgalactosaminyltransferases: completion of the family tree. *Glycobiology* **22,** 768–777
13. Peng, C., Togayachi, A., Kwon, Y. D., Xie, C., Wu, G., Zou, X., Sato, T., Ito, H., Tachibana, K., Kubota, T., Noce, T., Narimatsu, H., and Zhang, Y. (2010) Identification of a novel human UDP-GalNAc transferase with unique catalytic activity and expression profile. *Biochem. Biophys. Res. Commun.* **402,** 680–686
14. Bennett, E. P., Mandel, U., Clausen, H., Gerken, T. A., Fritz, T. A., and Tabak, L. A. (2012) Control of mucin-type *O*-glycosylation: a classification of the polypeptide GalNAc-transferase gene family. *Glycobiology* **22,** 736–756
15. Young, W. W., Jr, Holcomb, D. R., Ten Hagen, K. G., and Tabak, L. A. (2003) Expression of UDP-GalNAc:polypeptide *N*-acetylgalactosaminyltransferase isoforms in murine tissues determined by real-time PCR: a new view of a large family. *Glycobiology* **13,** 549–557
16. Tabak, L. A. (2010) The role of mucin-type *O*-glycans in eukaryotic development. *Semin. Cell Dev. Biol.* **21,** 616–621
17. Tran, D. T., and Ten Hagen, K. G. (2013) Mucin-type *O*-glycosylation during development. *J. Biol. Chem.* **288,** 6921–6929
18. Tenno, M., Ohtsubo, K., Hagen, F. K., Ditto, D., Zarbock, A., Schaerli, P., von Andrian, U. H., Ley, K., Le, D., Tabak, L. A., and Marth, J. D. (2007) Initiation of protein *O* glycosylation by the polypeptide GalNAcT-1 in vascular biology and humoral immunity. *Mol. Cell. Biol.* **27,** 8783–8796
19. Tian, E., Hoffman, M. P., and Ten Hagen, K. G. (2012) *O*-glycosylation modulates integrin and FGF signalling by influencing the secretion of basement membrane components. *Nat. Commun.* **3,** 869
20. Herr, P., Korniychuk, G., Yamamoto, Y., Grubisic, K., and Oelgeschläger, M. (2008) Regulation of TGF-β signalling by *N*-acetylgalactosaminyltransferase-like 1. *Development* **135,** 1813–1822
21. Boskovski, M. T., Yuan, S., Pedersen, N. B., Goth, C. K., Makova, S., Clausen, H., Brueckner, M., and Khokha, M. K. (2013) The heterotaxy gene GALNT11 glycosylates Notch to orchestrate cilia type and laterality. *Nature* **504,** 456–459
22. Takasaki, N., Tachibana, K., Ogasawara, S., Matsuzaki, H., Hagiuda, J., Ishikawa, H., Mochida, K., Inoue, K., Ogonuki, N., Ogura, A., Noce, T., Ito, C., Toshimori, K., and Narimatsu, H. (2014) A heterozygous mutation of GALNTL5 affects male infertility with impairment of sperm motility. *Proc. Natl. Acad. Sci. U.S.A.* **111,** 1120–1125
23. Kathiresan, S., Melander, O., Guiducci, C., Surti, A., Burtt, N. P., Rieder, M. J., Cooper, G. M., Roos, C., Voight, B. F., Havulinna, A. S., Wahlstrand, B., Hedner, T., Corella, D., Tai, E. S., Ordovas, J. M., *et al.* (2008) Six new loci associated with blood low-density lipoprotein cholesterol, high-density lipoprotein cholesterol or triglycerides in humans. *Nat. Genet.* **40,** 189–197
24. Willer, C. J., Sanna, S., Jackson, A. U., Scuteri, A., Bonnycastle, L. L., Clarke, R., Heath, S. C., Timpson, N. J., Najjar, S. S., Stringham, H. M., Strait, J., Duren, W. L., Maschio, A., Busonero, F., Mulas, A., *et al.* (2008) Newly identified loci that influence lipid concentrations and risk of coronary artery disease. *Nat. Genet.* **40,** 161–169
25. Schjoldager, K. T., Vester-Christensen, M. B., Bennett, E. P., Levery, S. B., Schwientek, T., Yin, W., Blixt, O., and Clausen, H. (2010) *O*-glycosylation modulates proprotein convertase activation of angiopoietin-like protein 3: possible role of polypeptide GalNAc-transferase-2 in regulation of concentrations of plasma lipids. *J. Biol. Chem.* **285,** 36293–36303
26. Topaz, O., Shurman, D. L., Bergman, R., Indelman, M., Ratajczak, P., Mizrachi, M., Khamaysi, Z., Behar, D., Petronius, D., Friedman, V., Zelikovic, I., Raimer, S., Metzker, A., Richard, G., and Sprecher, E. (2004) Mutations in GALNT3, encoding a protein involved in *O*-linked glycosylation, cause familial tumoral calcinosis. *Nat. Genet.* **36,** 579–581
27. Berois, N., Blanc, E., Ripoche, H., Mergui, X., Trajtenberg, F., Cantais, S., Barrois, M., Dessen, P., Kågedal, B., Bénard, J., Osinaga, E., and Raguénez, G. (2006) ppGalNAc-T13: a new molecular marker of bone marrow involvement in neuroblastoma. *Clin. Chem.* **52,** 1701–1712
28. Zhang, Y., Iwasaki, H., Wang, H., Kudo, T., Kalka, T. B., Hennet, T., Kubota, T., Cheng, L., Inaba, N., Gotoh, M., Togayachi, A., Guo, J., Hisatomi, H., Nakajima, K., Nishihara, S., *et al.* (2003) Cloning and characterization of a new human UDP-*N*-acetyl-α-D-galactosamine:polypeptide *N*-acetylgalactosaminyltransferase, designated pp-GalNAc-T13, that is specifically expressed in neurons and synthesizes GalNAc α-serine/threonine antigen. *J. Biol. Chem.* **278,** 573–584
29. Jones-Villeneuve, E. M., McBurney, M. W., Rogers, K. A., and Kalnins, V. I. (1982) Retinoic acid induces embryonal carcinoma cells to differentiate into neurons and glial cells. *J. Cell Biol.* **94,** 253–262
30. Jones-Villeneuve, E. M., Rudnicki, M. A., Harris, J. F., and McBurney, M. W. (1983) Retinoic acid-induced neural differentiation of embryonal carcinoma cells. *Mol. Cell. Biol.* **3,** 2271–2279
31. Resende, R. R., Majumder, P., Gomes, K. N., Britto, L. R., and Ulrich, H. (2007) P19 embryonal carcinoma cells as in vitro model for studying purinergic receptor expression and modulation of *N*-methyl-D-aspartate-glutamate and acetylcholine receptors during neuronal differentiation. *Neuroscience* **146,** 1169–1181
32. MacPherson, P. A., and McBurney, M. W. (1995) P19 embryonal carcinoma cells: a source of cultured neurons amenable to genetic manipulation. *Methods* **7,** 238–252
33. Kotani, M., Osanai, T., Tajima, Y., Kato, H., Imada, M., Kaneda, H., Kubo, H., and Sakuraba, H. (2002) Identification of neuronal cell lineage-specific molecules in the neuronal differentiation of P19 EC cells and mouse central nervous system. *J. Neurosci. Res.* **67,** 595–606
34. Kotani, M., Tajima, Y., Osanai, T., Irie, A., Iwatsuki, K., Kanai-Azuma, M., Imada, M., Kato, H., Shitara, H., Kubo, H., and Sakuraba, H. (2003) Complementary DNA cloning and characterization of RANDAM-2, a type I membrane molecule specifically expressed on glutamatergic neuronal cells in the mouse cerebrum. *J. Neurosci. Res.* **73,** 603–613
35. Schjoldager, K. T., Joshi, H. J., Kong, Y., Goth, C. K., King, S. L., Wandall, H. H., Bennett, E. P., Vakhrushev, S. Y., and Clausen, H. (2015) Deconstruction of *O*-glycosylation-GalNAc-T isoforms directly distinct subsets of the *O*-glycoproteome. *EMBO Rep.* **16,** 1713–1722
36. Kozarsky, K., Kingsley, D., and Krieger, M. (1988) Use of a mutant cell line to study the kinetics and function of *O*-linked glycosylation of low density lipoprotein receptors. *Proc. Natl. Acad. Sci. U.S.A.* **85,** 4335–4339
37. Reddy, P., Caras, I., and Krieger, M. (1989) Effects of *O*-linked glycosylation on the cell surface expression and stability of decay-accelerating factor, a glycophospholipid-anchored membrane protein. *J. Biol. Chem.* **264,** 17329–17336
38. Altschuler, Y., Kinlough, C. L., Poland, P. A., Bruns, J. B., Apodaca, G., Weisz, O. A., and Hughey, R. P. (2000) Clathrin-mediated endocytosis of MUC1 is modulated by its glycosylation state. *Mol. Biol. Cell* **11,** 819–831

39. Park, M., and Tenner, A. J. (2003) Cell surface expression of C1qRP/CD93 is stabilized by *O*-glycosylation. *J. Cell. Physiol.* **196,** 512–522
40. Kingsley, D. M., Kozarsky, K. F., Hobbie, L., and Krieger, M. (1986) Reversible defects in *O*-linked glycosylation and LDL receptor expression in a UDP-Gal/UDP-GalNAc 4-epimerase-deficient mutant. *Cell* **44,** 749–759
41. Voglmeir, J., Laurent, N., Flitsch, S. L., Oelgeschläger, M., and Wilson, I. B. (2015) Biological and biochemical properties of two *Xenopus laevis N*-acetylgalactosaminyltransferases with contrasting roles in embryogenesis. *Comp. Biochem. Physiol. B Biochem. Mol. Biol.* **180,** 40–47
42. Xuan, S., Baptista, C. A., Balas, G., Tao, W., Soares, V. C., and Lai, E. (1995) Winged helix transcription factor BF-1 is essential for the development of the cerebral hemispheres. *Neuron* **14,** 1141–1152
43. Lee, J. E. (1997) Basic helix-loop-helix genes in neural development. *Curr. Opin. Neurobiol.* **7,** 13–20
44. Wegner, M., and Stolt, C. C. (2005) From stem cells to neurons and glia: a Soxist's view of neural development. *Trends Neurosci.* **28,** 583–588
45. Thompson, J. A., Zembrzycki, A., Mansouri, A., and Ziman, M. (2008) Pax7 is requisite for maintenance of a subpopulation of superior collicular neurons and shows a diverging expression pattern to Pax3 during superior collicular development. *BMC Dev. Biol.* **8,** 62
46. White, R. B., and Ziman, M. R. (2008) Genome-wide discovery of Pax7 target genes during development. *Physiol. Genomics* **33,** 41–49
47. Ziman, M. R., Thomas, M., Jacobsen, P., and Beazley, L. (2001) A key role for Pax7 transcripts in determination of muscle and nerve cells. *Exp. Cell Res.* **268,** 220–229
48. Miller, F. D., and Gauthier, A. S. (2007) Timing is everything: making neurons versus glia in the developing cortex. *Neuron* **54,** 357–369
49. Bain, G., Ray, W. J., Yao, M., and Gottlieb, D. I. (1994) From embryonal carcinoma cells to neurons: the P19 pathway. *BioEssays* **16,** 343–348
50. Yao, M., Bain, G., and Gottlieb, D. I. (1995) Neuronal differentiation of P19 embryonal carcinoma cells in defined media. *J. Neurosci. Res.* **41,** 792–804
51. Herzog, B. H., Fu, J., Wilson, S. J., Hess, P. R., Sen, A., McDaniel, J. M., Pan, Y., Sheng, M., Yago, T., Silasi-Mansat, R., McGee, S., May, F., Nieswandt, B., Morris, A. J., Lupu, F., *et al.* (2013) Podoplanin maintains high endothelial venule integrity by interacting with platelet CLEC-2. *Nature* **502,** 105–109
52. Astarita, J. L., Acton, S. E., and Turley, S. J. (2012) Podoplanin: emerging functions in development, the immune system, and cancer. *Front. Immunol.* **3,** 283
53. Grau, S. J., Trillsch, F., Tonn, J. C., Goldbrunner, R. H., Noessner, E., Nelson, P. J., and von Luettichau, I. (2015) Podoplanin increases migration and angiogenesis in malignant glioma. *Int. J. Clin. Exp. Pathol.* **8,** 8663–8670
54. Pan, Y., Yago, T., Fu, J., Herzog, B., McDaniel, J. M., Mehta-D'Souza, P., Cai, X., Ruan, C., McEver, R. P., West, C., Dai, K., Chen, H., and Xia, L. (2014) Podoplanin requires sialylated *O*-glycans for stable expression on lymphatic endothelial cells and for interaction with platelets. *Blood* **124,** 3656–3665
55. Kaneko, M. K., Kato, Y., Kitano, T., and Osawa, M. (2006) Conservation of a platelet activating domain of Aggrus/podoplanin as a platelet aggregation-inducing factor. *Gene* **378,** 52–57
56. Kaneko, M. K., Kato, Y., Kameyama, A., Ito, H., Kuno, A., Hirabayashi, J., Kubota, T., Amano, K., Chiba, Y., Hasegawa, Y., Sasagawa, I., Mishima, K., and Narimatsu, H. (2007) Functional glycosylation of human podoplanin: glycan structure of platelet aggregation-inducing factor. *FEBS Lett.* **581,** 331–336
57. Suzuki-Inoue, K. (2009) CLEC-2, the novel platelet activation receptor and its internal ligand, podoplanin. *Rinsho Ketsueki* **50,** 389–398
58. Gerken, T. A., Revoredo, L., Thome, J. J., Tabak, L. A., Vester-Christensen, M. B., Clausen, H., Gahlay, G. K., Jarvis, D. L., Johnson, R. W., Moniz, H. A., and Moremen, K. (2013) The lectin domain of the polypeptide GalNAc transferase family of glycosyltransferases (ppGalNAc Ts) acts as a switch directing glycopeptide substrate glycosylation in an N- or C-terminal direction, further controlling mucin type *O*-glycosylation. *J. Biol. Chem.* **288,** 19900–19914
59. Revoredo, L., Wang, S., Bennett, E. P., Clausen, H., Moremen, K. W., Jarvis, D. L., Ten Hagen, K. G., Tabak, L. A., and Gerken, T. A. (2016) Mucin-type *O*-glycosylation is controlled by short- and long-range glycopeptide substrate recognition that varies among members of the polypeptide GalNAc transferase family. *Glycobiology* **26,** 360–376
60. Kong, Y., Joshi, H. J., Schjoldager, K. T., Madsen, T. D., Gerken, T. A., Vester-Christensen, M. B., Wandall, H. H., Bennett, E. P., Levery, S. B., Vakhrushev, S. Y., and Clausen, H. (2015) Probing polypeptide GalNAc-transferase isoform substrate specificities by *in vitro* analysis. *Glycobiology* **25,** 55–65
61. Matsumoto, Y., Zhang, Q., Akita, K., Nakada, H., Hamamura, K., Tokuda, N., Tsuchida, A., Matsubara, T., Hori, T., Okajima, T., Furukawa, K., Urano, T., and Furukawa, K. (2012) pp-GalNAc-T13 induces high metastatic potential of murine Lewis lung cancer by generating trimeric Tn antigen. *Biochem. Biophys. Res. Commun.* **419,** 7–13
62. Matsumoto, Y., Zhang, Q., Akita, K., Nakada, H., Hamamura, K., Tsuchida, A., Okajima, T., Furukawa, K., Urano, T., and Furukawa, K. (2013) Trimeric Tn antigen on syndecan 1 produced by ppGalNAc-T13 enhances cancer metastasis via a complex formation with integrin $\alpha5\beta1$ and matrix metalloproteinase 9. *J. Biol. Chem.* **288,** 24264–24276
63. Hienola, A., Tumova, S., Kulesskiy, E., and Rauvala, H. (2006) *N*-syndecan deficiency impairs neural migration in brain. *J. Cell Biol.* **174,** 569–580
64. Yamaguchi, Y. (2001) Heparan sulfate proteoglycans in the nervous system: their diverse roles in neurogenesis, axon guidance, and synaptogenesis. *Semin. Cell Dev. Biol.* **12,** 99–106
65. Monlauzeur, L., Breuza, L., and Le Bivic, A. (1998) Putative *O*-glycosylation sites and a membrane anchor are necessary for apical delivery of the human neurotrophin receptor in Caco-2 cells. *J. Biol. Chem.* **273,** 30263–30270
66. Kitazume, S., Tachida, Y., Kato, M., Yamaguchi, Y., Honda, T., Hashimoto, Y., Wada, Y., Saito, T., Iwata, N., Saido, T., and Taniguchi, N. (2010) Brain endothelial cells produce amyloid β from amyloid precursor protein 770 and preferentially secrete the *O*-glycosylated form. *J. Biol. Chem.* **285,** 40097–40103
67. Zamze, S., Harvey, D. J., Pesheva, P., Mattu, T. S., Schachner, M., Dwek, R. A., and Wing, D. R. (1999) Glycosylation of a CNS-specific extracellular matrix glycoprotein, tenascin-R, is dominated by *O*-linked sialylated glycans and "brain-type" neutral *N*-glycans. *Glycobiology* **9,** 823–831
68. Suzuki, M., Angata, K., Nakayama, J., and Fukuda, M. (2003) Polysialic acid and mucin type *O*-glycans on the neural cell adhesion molecule differentially regulate myoblast fusion. *J. Biol. Chem.* **278,** 49459–49468
69. Delgado-Esteban, M., García-Higuera, I., Maestre, C., Moreno, S., and Almeida, A. (2013) APC/C-Cdh1 coordinates neurogenesis and cortical size during development. *Nat. Commun.* **4,** 2879